

# Mechanosensitive Osteogenesis on Native Cellulose Scaffolds for Bone Tissue Engineering.

Maxime Leblanc Latour<sup>1</sup> and Andrew E. Pelling<sup>1,2,3</sup>

<sup>1</sup> Department of Physics, STEM Complex, 150 Louis Pasteur, University of Ottawa, Ottawa, ON, K1N 6N5, Canada

<sup>2</sup> Department of Biology, Gendron Hall, 30 Marie Curie, University of Ottawa, Ottawa, ON, K1N 6N5, Canada

<sup>3</sup> Institute for Science, Society and Policy, Desmarais Building, 55 Laurier Ave. East, University of Ottawa, Ottawa, ON, K1N 6N5, Canada

Author for correspondence: [a@pellinglab.net](mailto:a@pellinglab.net).

## Abstract

In recent years, plant-derived cellulosic biomaterials have become a popular way to create scaffolds for a variety of tissue engineering applications. Moreover, such scaffolds possess similar physical properties (porosity, stiffness) that resemble bone tissues and have been explored as potential biomaterials for tissue engineering applications. Here, plant-derived cellulose scaffolds were seeded with MC3T3-E1 pre-osteoblast cells. Moreover, to assess the potential these biomaterials we also applied cyclic hydrostatic pressure (HP) to the cells and scaffolds over time to mimic a bone-like environment more closely. After one week of proliferation, cell-seeded scaffolds were exposed to HP up to 270 KPa at a frequency of 1Hz, once per day, for up to two weeks. Scaffolds were incubated in osteogenic inducing media (OM) or regular culture media (CM). The effect of cyclic HP combined with OM on cell-seeded scaffolds resulted in an increase of differentiated cells. This corresponded with an upregulation of alkaline phosphatase activity and scaffold mineralization. The results reveal that in vitro, the mechanosensitive pathways which regulate osteogenesis appear to be functional on novel plant-derived cellulosic biomaterials.

## Introduction

Upon injury or break, bone has the ability to self-renew. However, large defects created by either injury or disease may require graft placement to avoid non-union or malunion of the bone tissue (Andrzejowski and Giannoudis, 2019). Such grafts can be derived directly from the patient (autologous grafts), and is considered the “gold standard” in regenerative orthopedics (Campana et al., 2014; Parikh, 2002; Sakkas et al., 2017; Wang and Yeung, 2017). However, limited size grafts, donor site morbidity and infections, cost and post-operative pain at both donor and receiver site has led to the development of alternative approaches (Parikh, 2002; Wang and Yeung, 2017): cadaver donors (allograft), animal sources (xenograft), or artificially derived (alloplastic). Such alternatives all have their own benefits and drawbacks, the later however provides a potential alternative with lower risk of transmitted diseases and infections, as well as overcoming the size limitation barrier (Parikh, 2002; Wang and Yeung, 2017).

47 Alloplastic grafts are also considered a more ethical alternative to allografts and xenografts  
48 (Fernández et al., 2015). Physical properties are key parameters for graft development, such as  
49 pore size, interconnectivity and elasticity (Campana et al., 2014; Gao et al., 2019; Nukavarapu  
50 et al., 2015). Fine tuning of these parameters leads to better mechanical support and stability of  
51 the implant.

52  
53 Long bones are highly dynamic structural tissues. A whole spectrum of forces are acting on  
54 different areas of this part of the skeletal system. For instance, the pressure found in the femur  
55 head in human adults can reach 5 MPa during normal locomotion, and can reach up to 18 MPa  
56 for other activities (Morrell et al., 2005). On a microscopic level, these forces are transmitted to  
57 the osteocytes through Wnt/ $\beta$ -catenin mechano-sensing pathways in the lacuna-canalicular  
58 network (Bonewald and Johnson, 2008). Force-regulated mechanisms lead to formation and  
59 removal of bone tissue through bone remodeling processes (Bonewald and Johnson, 2008) and  
60 the pressure inside the lacuna-canalicular network is around 280 kPa (Zhang et al., 1998).  
61 Bioreactors have also been developed to apply stresses to osteoblast cells to replicate the  
62 native bone environment via uniaxial compression/tension, biaxial compression/tension, shear-  
63 stress, etc (Brunelli et al., 2019; Pörtner et al., 2005). Hydrostatic pressure (HP) stimulation on  
64 cultured cells has also been achieved by compressing the gas phase above an incompressible  
65 media (Gardinier et al., 2009; Henstock et al., 2013; Liu et al., 2010; Reinwald et al., 2015;  
66 Reinwald and El Haj, 2018; Stavenschi et al., 2018; Zhao et al., 2015). Three-dimensional (3D)  
67 culturing of the cells is also critical for better representing *in vivo* conditions. With a specific  
68 tissue-oriented scaffold structure and appropriate applied mechanical stimuli one can potentially  
69 predict the performance of a biomaterial scaffold prior to *in vivo* animal studies.

70  
71 A variety of 3D biomaterials have been utilized support the growth and proliferation of cells in  
72 environments that mimic bone tissues. These include hydroxyapatite, tricalcium phosphate,  
73 bioceramics or bioactive glass (Wang and Yeung, 2017). These materials are osteoconductive,  
74 can promote osteointegration and provide structural support at the implant site (Wang and  
75 Yeung, 2017). However, they show poor osteoconduction and little osteogenic response  
76 (Wang and Yeung, 2017). Polymer biomaterials such as poly(glycolic acid) (PGA), poly(lactic  
77 acid) (PLA) and poly( $\epsilon$ -caprolactone) (PCL) are also biocompatible, possess tunable  
78 degradation rates and can be chemically modify to change the surface chemistry (Wei et al.,  
79 2020). However, *in vivo* degradation creates acidic bi-products which can lead to an  
80 inflammatory response and decrease the efficiency bone repair (Wei et al., 2020). Finally,  
81 naturally occurring polymers such as collagen, chitosan and silk are also common (Wei et al.,  
82 2020). However, due to their inherent mechanical properties and structural stability, these  
83 materials are often utilized as composites with additional polymers and coatings in BTE  
84 applications (Di Martino et al., 2005; Lee and Volpicelli, 2017; Wei et al., 2020). More recently,  
85 plant-derived decellularized cellulose scaffolds have been shown to be effective in BTE  
86 applications (Hickey and Pelling, 2019; Lee et al., 2019; Torgbo and Sukyai, 2018).

87  
88 Previous studies by our group and others have shown that cellulose based scaffolds derived  
89 from plants can be used as tissue engineering scaffolds (Gershlak et al., 2017; Hickey et al.,  
90 2018; Lee et al., 2019; Modulevsky et al., 2016, 2014). These biomaterials are often sourced  
91 from plants with a microstructure that closely mimics the tissue to be replicated (Hickey et al.,  
92 2018). Successful experiments *in vitro* and *in vivo* showed that these biomaterials are  
93 biocompatible and support angiogenesis (Hickey et al., 2018; Modulevsky et al., 2016, 2014).  
94 Due to their pore size interconnectivity, other groups have successfully differentiated human  
95 pluripotent stem cells into bone-like tissues within scaffolds derived from either decellularized  
96 mushrooms (Balasundari et al., 2012) or apple tissues (Lee et al., 2019). The *in vivo*  
97 performance of the apple-derived scaffolds were further examined by implanting disk-shaped

98 scaffolds in rat cranial defects (Lee et al., 2019). The findings demonstrate partial bone  
99 regeneration within the implant, type 1 collagen deposition and blood vessel formation (Lee et  
100 al., 2019). However, to date, the mechanobiology of cells cultured on plant-derived scaffolds  
101 has not been examined. It remains poorly understood how mechanical signal transduction  
102 pathways are, or are not, impacted when cultured on unconventional plant-derived cellulosic  
103 biomaterials. Here, to further examine the potential role plant-based biomaterials can play in  
104 BTE applications, we explore how mechanical stimulation impacts the differentiation of pre-  
105 osteoblasts when cultured on plant cellulose scaffolds. In a custom-built bioreactor, we apply  
106 cyclic HP stimulation to differentiating osteoblasts and examine the regulation of key markers of  
107 osteogenesis and mineralization. The results reveal that application of HP, in combination with  
108 osteogenic inducing media, leads to enhanced differentiation. This work provides further  
109 evidence that plant-derived cellulose scaffolds support osteogenesis and have potential  
110 applications in BTE.

111

112

## 113 **Materials and Methods**

114

### 115 **Scaffold fabrication**

116

117 Samples were prepared following established protocols (Hickey et al., 2018; Modulevsky et al.,  
118 2016, 2014). MacIntosh apples (Canada Fancy) were cut with a mandolin slicer to 1 mm-thick  
119 slices. A biopsy punch was used to create 5 mm-diameter disks in the hypanthium tissue of the  
120 apple slices. The disks were decellularized in a 0.1% sodium dodecyl sulfate solution (SDS,  
121 Fisher Scientific, Fair Lawn, NJ) for two days. Then, the decellularized disks were washed in  
122 deionized water, before incubation in 100 mM CaCl<sub>2</sub> for two days. The samples were sterilized  
123 with 70% ethanol, washed in deionized water, and placed in a 96-well culture plate prior to cell  
124 seeding.

125

126 MC3T3-E1 Subclone 4 cells (ATCC® CRL-2593™, Manassas, VA) were cultured and  
127 maintained in a humidified atmosphere of 95% air and 5% CO<sub>2</sub>, at 37°C. The cells were cultured  
128 in Minimum Essential Medium (ThermoFisher, Waltham, MA), supplemented with 10% Fetal  
129 Bovine Serum (Hyclone Laboratories Inc., Logan, UT) and 1% Penicillin/Streptomycin (Hyclone  
130 Laboratories Inc). Scaffolds were placed in 96-well plates. Prior to cell seeding, scaffolds were  
131 immersed in culture media and incubated in a humidified atmosphere of 95% air and 5% CO<sub>2</sub>, at  
132 37°C, for 30 min. The culture media was completely aspirated from the wells. Cells were  
133 suspended and a 30 µL drop containing 5 x 10<sup>4</sup> cells, was pipetted on each scaffold. The cells  
134 were left to adhere on the scaffolds for 2 hours before adding 200 µL of culture media to the  
135 culture wells. Culture media was then changed every 3-4 days for 1 week. Cell seeded scaffolds  
136 were then either incubated in osteogenic media (OM) by adding 50 µg/mL of ascorbic acid and  
137 10 mM β-glycerophosphate to the culture media or incubated in culture media (CM) for 2 weeks,  
138 with or without the application of HP.

139

### 140 **Cyclic hydrostatic pressure stimulation**

141

142 Cyclic HP was applied by modulating the pressure in the gas phase above the culture wells in a  
143 custom-build pressure chamber (Figure 1, A). The humidified, 95% air and 5% CO<sub>2</sub> incubator  
144 atmosphere was compressed using an air compressor and injected in the chamber. A Particle  
145 Photon microcontroller (Particle Industries, San Francisco, CA) was used to control the  
146 frequency of the applied pressure remotely via a custom-made cellphone application through  
147 the Blynk IoT platform (Blynk, New York, NY)). Cyclic HP was applied 1 hour per day, for up to 2

148 weeks (Figure 1, B) at a frequency 1Hz, oscillating between 0 and 280 kPa with respect to  
149 ambient pressure. Pressure was monitored using a pressure transducer. The samples were  
150 removed from the pressure chamber after each cycle and kept at ambient pressure between the  
151 stimulation phases.

152  
153 Cell-seeded scaffolds were either stimulated with cyclic HP with and without the presence of  
154 OM, leading to four experimental conditions (Figure 1, B): Cyclic HP in regular culture media  
155 (CM-HP), cyclic HP in osteogenic culture media (OM-HP), non-stimulated in osteogenic media  
156 (OM-CTRL) and non-stimulated in regular culture media (CM-CTRL). The OM-CTRL and CM-  
157 CTRL conditions were in a humidified, 5% CO<sub>2</sub> incubator at 37°C.

158  
159 **Scaffold imaging**

160  
161 After 1 week or 2 weeks, scaffolds were washed with PBS and fixed with 10% neutral buffered  
162 formalin for 10 min. Scaffolds were washed with PBS and incubated in a 0.01% Congo Red  
163 staining solution (Sigma-Aldrich, St. Louis, MO) for 20 min at room temperature. Scaffolds were  
164 washed with PBS. Cell nuclei were stained with 1:1000 Hoechst (ThermoFisher, Waltham, MA)  
165 for 30 min in the dark. Samples were washed with PBS and stored in wash buffer solution (5%  
166 FBS in PBS) prior to imaging. The cell-seeded surface of the scaffolds was imaged with a laser  
167 scanning confocal microscope (Nikon Ti-E A1-R) equipped with a 10X objective. Maximum  
168 intensity projections were used for cell counting with ImageJ software (Schindelin et al., 2012).  
169 Cells were counted on a 1.3 by 1.3 mm<sup>2</sup> area (N=3 per experimental conditions with 3 randomly  
170 selected area per scaffold).

171  
172 **Alkaline phosphatase activity assay**

173  
174 Alkaline phosphatase (ALP) activity in media was measured using an ALP assay kit (BioAssay  
175 Systems, Hayward, CA). Working solution was prepared with 5 mM magnesium acetate and 10  
176 mM p-nitrophenyl phosphate (pNPP) in assay buffer, following manufacturer's protocol. 150 µL  
177 of working solution was pipetted in 96-well plate. 200 µL of calibrator solution and 200 µL of  
178 dH<sub>2</sub>O were pipetted in separated well, in the same 96-well plate. At 1 week and 2 weeks, 20 µL  
179 of incubation media was pipetted into the working solution's well. All wells were read at 405 nm  
180 for 10 minutes, every 30 seconds. ALP activity was calculated by taking the slope of the 405 nm  
181 readings vs time, calibrated with the calibrator solution and dH<sub>2</sub>O. Wells were read in triplicates  
182 (N=3 per experimental conditions).

183  
184 **Alizarin red S staining and mineral deposit quantification**

185  
186 Samples were fixed with 10% neutral buffered formalin for 10 min, after 1 week or 2 weeks.  
187 Calcium quantification was performed using previously published protocol (Gregory et al.,  
188 2004). Samples were transferred to a 24-well plate and carefully washed with deionized water  
189 and incubated in 1 mL of 40mM (pH=4.1) alizarin red s (ARS, Sigma-Aldrich) solution for 20  
190 minutes at room temperature, with light agitation. The samples were washed with deionized  
191 water and placed in 15 mL tubes filled with 10 mL dH<sub>2</sub>O. The tubes were placed on a rotary  
192 shaker at 120 rpm for 60 min and dH<sub>2</sub>O was replaced every 15 min. Thereafter, samples were  
193 incubated in 800 µL of 10% acetic acid on an orbital shaker at 60 rpm for 30 min. The eluted  
194 ARS/acetic acid solution was pipettes out of the well and transferred to 1.5 mL centrifuge tubes.  
195 Tubes were centrifuged at 17 x 10<sup>4</sup> g for 15 min. 500 µL of supernatants were transferred to  
196 new centrifuge tube and 200 µL of 10% ammonium hydroxide was pipetted into the tubes.  
197 Finally, 150 µL of the solution was pipetted into a 96-well plate and the absorption at 405nm

198 was read using a plate reader (BioTek Instruments, Winooski, VT). Wells were read in triplicates  
199 (N=3 per experimental conditions).

200

## 201 **Statistical analysis**

202

203 Values reported in this manuscript are the average value  $\pm$  standard error of the mean (SEM).  
204 Statistical significance was determined using one-way ANOVA and post hoc Tukey test. A value  
205 of  $p < 0.05$  was considered to be statistically significant.

206

207

## 208 **Results**

### 209 **Scaffold imaging and cell counting**

210

211 Mechanical stimulation of the cultured scaffolds was carried as described in the Methods  
212 (Figure 1). The application of HP significantly increases the density of cells (Figure 2) after 1  
213 week in OM compared to the static condition ( $p=10^{-5}$ ), but the increase was not significant after  
214 2 weeks ( $p=0.07$ ). Conversely, in CM a non-significant increase in the density of cells was  
215 observed with applied HP after 1 week ( $p=0.21$ ) and 2 weeks ( $p=0.92$ ). Importantly, we also  
216 observed a significant increase when incubated in OM compared to CM after 1 week of HP  
217 stimulation ( $p=0.02$ ). After 2 weeks of HP stimulation, samples cultured in OM exhibited a  
218 similar density to samples cultured in CM ( $p=0.23$ ). The results indicate that cell density  
219 increases more rapidly in the first week of stimulation in OM compared to CM media but that by  
220 two weeks the cell densities become equal. No significant difference was observed in the static  
221 cases after 1 or 2 weeks ( $p=0.99$  in both cases).

222

### 223 **Alkaline phosphatase activity assay**

224

225 The stimulation with cyclic HP significantly increased the ALP activity (Figure 3) in scaffolds  
226 incubated in OM after 1 and 2 weeks compared to static condition ( $p=4 \times 10^{-8}$  in both cases). A  
227 similar effect was observed in CM after 1 and 2 weeks ( $p=0.03$  and  $p=5 \times 10^{-8}$  respectively).  
228 However, the incubation in OM significantly increased ALP activity when HP is applied  
229 compared to incubation in CM, after 1 week ( $p < 10^{-8}$ ) but was not significantly different after 2  
230 weeks ( $p=0.99$ ). Consistent with the cell density data the HP-driven increases in ALP activity  
231 are only observed during the first week and equalize by the second week of culture. In the  
232 absence of HP, the choice of incubation media did not significantly change the ALP activity after  
233 1 or 2 weeks ( $p=0.25$  and  $p=0.08$  respectively).

234

### 235 **Alizarin red S staining and mineral deposit quantification**

236

237 The application of cyclic HP significantly increased mineral deposition (Figure 4) for samples  
238 incubated in OM compared to static condition after 1 week and 2 weeks ( $p=2 \times 10^{-7}$  and  $p=2 \times 10^{-8}$   
239 respectively). Similarly in samples cultured in CM, cyclic HP significantly increased mineral  
240 deposition after 1 week and 2 weeks ( $p=1 \times 10^{-6}$  and  $p=2 \times 10^{-8}$  respectively). Moreover, the  
241 incubation in OM significantly increased mineral deposition when HP is applied compared to  
242 incubation in CM, after 1 week ( $p=2 \times 10^{-4}$ ), but was not significant after 2 weeks ( $p=0.99$ ). These  
243 results are again consistent with the findings from assays of cell density and ALP activity. Under  
244 static conditions mineralization still occurred in OM as expected and was significantly increased  
245 compared to CM after 1 week ( $p=10^{-3}$ ), but was not significant after 2 weeks ( $p=0.75$ ).

246

247  
248  
249  
250

## 251 Discussion

252

253 Cells utilize a variety of mechanisms to sense and respond to a variety of mechanical stimuli  
254 (Vining and Mooney, 2017). Mechanical stimuli are known to affect cell differentiation, tissue  
255 regeneration, cytokines and protein expression and proliferation (Martino et al., 2018; Vining  
256 and Mooney, 2017). Thus, adequate representation of physical environment is critical in implant  
257 design (Campana et al., 2014; Gao et al., 2019; Nukavarapu et al., 2015; Parikh, 2002; Wang  
258 and Yeung, 2017). Bones are subjected to constant mechanical stresses and adapt through  
259 remodeling process (Bonewald and Johnson, 2008). *In vivo*, HP stimulates bone cells and  
260 impacts cell differentiation, marker expression and mineralisation (Henstock et al., 2013; Huang  
261 and Ogawa, 2012; Reinwald and El Haj, 2018). Plant-derived cellulose scaffolds are an  
262 emerging biomaterial in BTE (Lee et al., 2019), and therefore it is of interest to understand their  
263 performance under the mechanical conditions that are found *in vivo* (Gao et al., 2019;  
264 Nukavarapu et al., 2015). To our knowledge, cyclic HP effect of pre-osteoblasts seeded on  
265 plant-derived scaffolds have not yet been studied. Cellulose biomaterials derived from plant  
266 tissues have shown promising results *in vitro* and *in vivo* for targeted tissue engineering (Hickey  
267 et al., 2018; Modulevsky et al., 2016, 2014) and have been used to host osteoblastic  
268 differentiation (Lee et al., 2019). In addition, apple-derived cellulose scaffolds exhibit similar  
269 morphological characteristics to trabecular bone and were previously used for BTE applications  
270 (Lee et al., 2019).

271

272 In this study, we replicated the mechanical stimuli present during human locomotion by  
273 measuring the impact of differentiation markers in cellulose scaffolds seeded with pre-osteoblast  
274 cells. External pressure was applied on the scaffolds in similar magnitude of the lacuna-  
275 canaliculi network with a frequency mimicking human locomotion (Henstock et al., 2013; Zhang  
276 et al., 1998). After proliferation, our scaffolds were either cultured in standard culture media, or  
277 in osteogenic-inducing differentiation media, with or without high pressure stimulation. Other  
278 groups utilizing similar cell lines (Gardinier et al., 2014, 2009), bone marrow skeletal stem cells  
279 (Reinwald and El Haj, 2018; Stavenschi et al., 2018; Zhao et al., 2015) or ex-vivo chick femur  
280 (Henstock et al., 2013) have also studied the effects of cyclic HP on either 2D surfaces,  
281 biomaterial meshes or ex vivo bones. In general, our results show a sensitivity of HP during the  
282 early differentiation of the cells during the first week of stimulation. This sensitivity largely  
283 subsides during the second week of culture.

284

285 Cell counting revealed that the application of HP enhances MC3T3-E1 proliferation when  
286 cultured in OM or CM. Consistent with our work, are the results from previous studies in which  
287 metabolic activity has also been shown to be upregulated by mechanical stimulation in  
288 comparison to non-stimulated samples (Reinwald and El Haj, 2018). Moreover, it was shown  
289 that the application of HP accelerates cell proliferation through upregulated cell cycle initiation  
290 (Zhao et al., 2015). Similarly, reports have shown that physical stimulation of MC3T3-E1 cells  
291 induced expression of paracrine factors that leads enhancement of cell proliferation (Stavenschi  
292 et al., 2018). Importantly, when cultured in OM, cell density increases more rapidly with HP  
293 compared to CM during the first week of culture, but the cell densities equalize by the end of the  
294 second week. This data is consistent with previous reports of a time-dependent increase in cell  
295 number when cultured in OM (Quarles et al., 1992). Similarly, no significant difference between  
296 incubation of MC3T3-E1 cells in similar OM after 2 weeks (Hong et al., 2010). Our findings

297 corroborate these studies and further suggest that the application of HP influences the  
298 replication rate at early stages of stimulation for samples cultured in OM.

299  
300 Finally, ALP is an important enzyme expressed in the early stages of osteoblastic differentiation  
301 (Golub and Boesze-Battaglia, 2007). Our results indicate that the application of cyclic HP  
302 significantly increases ALP activity, compared to the static case. These findings are consistent  
303 with other studies on more conventional scaffolds (Reinwald and El Haj, 2018). For example, a  
304 significant increase in ALP activity was also reported after the incubation of scaffolds in  
305 osteogenic-inducing differentiation media, similarly to reports on 2D culture systems (Hong et  
306 al., 2010; Quarles et al., 1992). The application of HP significantly increased the mineral  
307 content in the scaffolds after 1 week and 2 weeks of stimulation, in both types of incubation  
308 media. Other groups have shown that a cyclic 300 kPa pressure at 2 Hz frequency on human  
309 BMSCs promoted significant mineral deposition (Stavenschi et al., 2018). The increase in  
310 mineral deposition also noted in *ex vivo* bone samples, with similar HP force application  
311 (Henstock et al., 2013). Furthermore, the incubation in OM increased the mineral content in the  
312 scaffolds, which is consistent with other studies (Hong et al., 2010; Quarles et al., 1992). Along  
313 with ALP expression, mineral content expression further confirms the ongoing differentiation of  
314 MC3T3-E1 onto osteoblast, either by applied HP, chemically (induction in OM) or a combination  
315 of both.

316  
317

## 318 **Conclusion**

319  
320 Plant-derived scaffolds have demonstrated their efficiency for tissue engineering applications  
321 (Fontana et al., 2017; Gershlak et al., 2017; Hickey et al., 2018; Lee et al., 2019; Modulevsky et  
322 al., 2016, 2014). The novelty, widespread availability, ease of use makes an interesting  
323 alternative to autografts, xenografts and synthetic implants. However, it has remained poorly  
324 understood how mechanosensitive pathways in bone precursor cells are impacted by being  
325 cultured in plant-derived cellulosic biomaterials. Previous studies have not included these  
326 phenomena. In this study, mechanical stimulation of cell-seeded scaffolds and the subsequent  
327 cellular response allowed us to understand the implants mechanosensitive behaviors in these  
328 novel scaffolds. As bone tissues are highly dynamic environments, relevant forces should be  
329 considered in the implant design. Importantly, this work provides the early evidence that bone-  
330 precursor cells appear to possess intact mechanosensing and mechanotransduction pathways  
331 when cultured on plant-derived scaffolds in a mechanically active environment. The results  
332 obtained here are consistent with data on traditional scaffold choices. The results reveal that  
333 application of cyclic HP, in combination with OM, leads to an increase in the number of cells,  
334 ALP activity and mineralization over time. These results combined with past *in vitro* and *in vivo*  
335 studies using apple-derived scaffold biomaterials demonstrate their potential in BTE  
336 applications.

337  
338

## 339 **Acknowledgements**

340  
341 This work was supported by a Discovery Grant from the Natural Sciences and Engineering  
342 Research Council of Canada (NSERC) and a grant from the Li Ka Shing Foundation.

343  
344

## 345 **References**

- 346  
347 Andrzejowski, P., Giannoudis, P. V., 2019. The “diamond concept” for long bone non-union  
348 management. *J. Orthop. Traumatol.* <https://doi.org/10.1186/s10195-019-0528-0>
- 349 Balasundari, R., Bishi, D.K., Mathapati, S., Naser, S.B., Cherian, K.M., Guhathakurta, S., 2012.  
350 Nanocoated botanical scaffold in salvage for human tissue regeneration. *J. Biomater.*  
351 *Tissue Eng.* 2, 330–335. <https://doi.org/10.1166/jbt.2012.1058>
- 352 Bonewald, L.F., Johnson, M.L., 2008. Osteocytes, mechanosensing and Wnt signaling. *Bone.*  
353 <https://doi.org/10.1016/j.bone.2007.12.224>
- 354 Brunelli, M., Perrault, C., Lacroix, D., 2019. A Review of Bioreactors and Mechanical Stimuli.  
355 Springer, Singapore, pp. 1–22. [https://doi.org/10.1007/978-981-10-8075-3\\_1](https://doi.org/10.1007/978-981-10-8075-3_1)
- 356 Campana, V., Milano, G., Pagano, E., Barba, M., Cicione, C., Salonna, G., Lattanzi, W.,  
357 Logroscino, G., 2014. Bone substitutes in orthopaedic surgery: from basic science to  
358 clinical practice. *J. Mater. Sci. Mater. Med.* 25, 2445–2461. [https://doi.org/10.1007/s10856-](https://doi.org/10.1007/s10856-014-5240-2)  
359 [014-5240-2](https://doi.org/10.1007/s10856-014-5240-2)
- 360 Di Martino, A., Sittinger, M., Risbud, M. V., 2005. Chitosan: A versatile biopolymer for  
361 orthopaedic tissue-engineering. *Biomaterials.*  
362 <https://doi.org/10.1016/j.biomaterials.2005.03.016>
- 363 Fernández, R.F., Bucchi, C., Navarro, P., Beltrán, V., Borie, E., 2015. Bone grafts utilized in  
364 dentistry: an analysis of patients’ preferences. *BMC Med. Ethics* 16, 71.  
365 <https://doi.org/10.1186/s12910-015-0044-6>
- 366 Fontana, G., Gershlak, J., Adamski, M., Lee, J.-S., Matsumoto, S., Le, H.D., Binder, B., Wirth,  
367 J., Gaudette, G., Murphy, W.L., 2017. Biofunctionalized Plants as Diverse Biomaterials for  
368 Human Cell Culture. *Adv. Healthc. Mater.* 6, 1601225.  
369 <https://doi.org/10.1002/adhm.201601225>
- 370 Gao, X., Fraulob, M., Haïat, G., 2019. Biomechanical behaviours of the bone-implant interface:  
371 A review. *J. R. Soc. Interface* 16, 20190259. <https://doi.org/10.1098/rsif.2019.0259>
- 372 Gardinier, J.D., Gangadharan, V., Wang, L., Duncan, R.L., 2014. Hydraulic pressure during fluid  
373 flow regulates purinergic signaling and cytoskeleton organization of osteoblasts. *Cell. Mol.*  
374 *Bioeng.* 7, 266–277. <https://doi.org/10.1007/s12195-014-0329-8>
- 375 Gardinier, J.D., Majumdar, S., Duncan, R.L., Wang, L., 2009. Cyclic hydraulic pressure and fluid  
376 flow differentially modulate cytoskeleton re-organization in MC3T3 osteoblasts. *Cell. Mol.*  
377 *Bioeng.* 2, 133–143. <https://doi.org/10.1007/s12195-008-0038-2>
- 378 Gershlak, J.R., Hernandez, S., Fontana, G., Perreault, L.R., Hansen, K.J., Larson, S.A., Binder,  
379 B.Y.K., Dolivo, D.M., Yang, T., Dominko, T., Rolle, M.W., Weathers, P.J., Medina-Bolivar,  
380 F., Cramer, C.L., Murphy, W.L., Gaudette, G.R., 2017. Crossing kingdoms: Using  
381 decellularized plants as perfusable tissue engineering scaffolds. *Biomaterials* 125, 13–22.  
382 <https://doi.org/10.1016/J.BIOMATERIALS.2017.02.011>
- 383 Golub, E.E., Boesze-Battaglia, K., 2007. The role of alkaline phosphatase in mineralization.  
384 *Curr. Opin. Orthop.* 18, 444–448. <https://doi.org/10.1097/BCO.0b013e3282630851>
- 385 Gregory, C.A., Gunn, W.G., Peister, A., Prockop, D.J., 2004. An Alizarin red-based assay of  
386 mineralization by adherent cells in culture: Comparison with cetylpyridinium chloride



- 387 extraction. *Anal. Biochem.* 329, 77–84. <https://doi.org/10.1016/j.ab.2004.02.002>
- 388 Henstock, J.R., Rotherham, M., Rose, J.B., El Haj, A.J., 2013. Cyclic hydrostatic pressure  
389 stimulates enhanced bone development in the foetal chick femur in vitro. *Bone* 53, 468–  
390 477. <https://doi.org/10.1016/j.bone.2013.01.010>
- 391 Hickey, R.J., Modulevsky, D.J., Cuerrier, C.M., Pelling, A.E., 2018. Customizing the Shape and  
392 Microenvironment Biochemistry of Biocompatible Macroscopic Plant-Derived Cellulose  
393 Scaffolds. *ACS Biomater. Sci. Eng.* 4, 3726–3736.  
394 <https://doi.org/10.1021/acsbiomaterials.8b00178>
- 395 Hickey, R.J., Pelling, A.E., 2019. Cellulose biomaterials for tissue engineering. *Front. Bioeng.*  
396 *Biotechnol.* <https://doi.org/10.3389/fbioe.2019.00045>
- 397 Hong, D., Chen, H.X., Yu, H.Q., Liang, Y., Wang, C., Lian, Q.Q., Deng, H.T., Ge, R.S., 2010.  
398 Morphological and proteomic analysis of early stage of osteoblast differentiation in  
399 osteoblastic progenitor cells. *Exp. Cell Res.* 316, 2291–2300.  
400 <https://doi.org/10.1016/j.yexcr.2010.05.011>
- 401 Huang, C., Ogawa, R., 2012. Effect of Hydrostatic Pressure on Bone Regeneration Using  
402 Human Mesenchymal Stem Cells. *Tissue Eng. Part A* 18, 2106–2113.  
403 <https://doi.org/10.1089/ten.tea.2012.0064>
- 404 Lee, J., Jung, H., Park, N., Park, S.H., Ju, J.H., 2019. Induced Osteogenesis in Plants  
405 Decellularized Scaffolds. *Sci. Rep.* 9, 1–10. <https://doi.org/10.1038/s41598-019-56651-0>
- 406 Lee, J.C., Volpicelli, E.J., 2017. Bioinspired Collagen Scaffolds in Cranial Bone Regeneration:  
407 From Bedside to Bench. *Adv. Healthc. Mater.* <https://doi.org/10.1002/adhm.201700232>
- 408 Liu, C., Zhao, Y., Cheung, W.Y., Gandhi, R., Wang, L., You, L., 2010. Effects of cyclic hydraulic  
409 pressure on osteocytes. *Bone* 46, 1449–1456. <https://doi.org/10.1016/j.bone.2010.02.006>
- 410 Martino, F., Perestrelo, A.R., Vinarský, V., Pagliari, S., Forte, G., 2018. Cellular  
411 mechanotransduction: From tension to function. *Front. Physiol.*  
412 <https://doi.org/10.3389/fphys.2018.00824>
- 413 Modulevsky, D.J., Cuerrier, C.M., Pelling, A.E., 2016. Biocompatibility of Subcutaneously  
414 Implanted Plant-Derived Cellulose Biomaterials. *PLoS One* 11, e0157894.  
415 <https://doi.org/10.1371/journal.pone.0157894>
- 416 Modulevsky, D.J., Lefebvre, C., Haase, K., Al-Rekabi, Z., Pelling, A.E., 2014. Apple derived  
417 cellulose scaffolds for 3D mammalian cell culture. *PLoS One* 9, e97835.  
418 <https://doi.org/10.1371/journal.pone.0097835>
- 419 Morrell, K.C., Hodge, W.A., Krebs, D.E., Mann, R.W., 2005. Corroboration of in vivo cartilage  
420 pressures with implications for synovial joint tribology and osteoarthritis causation. *Proc.*  
421 *Natl. Acad. Sci. U. S. A.* 102, 14819–14824. <https://doi.org/10.1073/pnas.0507117102>
- 422 Nukavarapu, S.P., Freeman, J.W., Laurencin, C.T., 2015. Regenerative Engineering of  
423 Musculoskeletal Tissues and Interfaces, *Regenerative Engineering of Musculoskeletal*  
424 *Tissues and Interfaces*. Elsevier Inc. <https://doi.org/10.1016/C2014-0-02826-2>
- 425 Parikh, S.N., 2002. Bone graft substitutes: past, present, future. *J. Postgrad. Med.* 48, 142–148.
- 426 Pörtner, R., Nagel-Heyer, S., Goepfert, C., Adamietz, P., Meenen, N.M., 2005. Bioreactor  
427 design for tissue engineering. *J. Biosci. Bioeng.* <https://doi.org/10.1263/jbb.100.235>

- 428 Quarles, L.D., Yohay, D.A., Lever, L.W., Caton, R., Wenstrup, R.J., 1992. Distinct proliferative  
429 and differentiated stages of murine MC3T3-E1 cells in culture: An in vitro model of  
430 osteoblast development. *J. Bone Miner. Res.* 7, 683–692.  
431 <https://doi.org/10.1002/jbmr.5650070613>
- 432 Reinwald, Y., El Haj, A.J., 2018. Hydrostatic pressure in combination with topographical cues  
433 affects the fate of bone marrow-derived human mesenchymal stem cells for bone tissue  
434 regeneration. *J. Biomed. Mater. Res. - Part A* 106, 629–640.  
435 <https://doi.org/10.1002/jbm.a.36267>
- 436 Reinwald, Y., Leonard, K.H.L., Henstock, J.R., Whiteley, J.P., Osborne, J.M., Waters, S.L.,  
437 Levesque, P., El Haj, A.J., 2015. Evaluation of the growth environment of a hydrostatic  
438 force bioreactor for preconditioning of tissue-engineered constructs. *Tissue Eng. - Part C*  
439 *Methods* 21, 1–14. <https://doi.org/10.1089/ten.tec.2013.0476>
- 440 Sakkas, A., Wilde, F., Heufelder, M., Winter, K., Schramm, A., 2017. Autogenous bone grafts in  
441 oral implantology—is it still a “gold standard”? A consecutive review of 279 patients with  
442 456 clinical procedures. *Int. J. Implant Dent.* 3. <https://doi.org/10.1186/s40729-017-0084-4>
- 443 Schindelin, J., Arganda-Carreras, I., Frise, E., Kaynig, V., Longair, M., Pietzsch, T., Preibisch,  
444 S., Rueden, C., Saalfeld, S., Schmid, B., Tinevez, J.-Y., White, D.J., Hartenstein, V.,  
445 Eliceiri, K., Tomancak, P., Cardona, A., 2012. Fiji: an open-source platform for biological-  
446 image analysis. *Nat. Methods* 9, 676–682. <https://doi.org/10.1038/nmeth.2019>
- 447 Stavenschi, E., Corrigan, M.A., Johnson, G.P., Riffault, M., Hoey, D.A., 2018. Physiological  
448 cyclic hydrostatic pressure induces osteogenic lineage commitment of human bone marrow  
449 stem cells: A systematic study. *Stem Cell Res. Ther.* 9. <https://doi.org/10.1186/s13287-018-1025-8>
- 451 Torgbo, S., Sukyai, P., 2018. Bacterial cellulose-based scaffold materials for bone tissue  
452 engineering. *Appl. Mater. Today* 11, 34–49. <https://doi.org/10.1016/J.APMT.2018.01.004>
- 453 Vining, K.H., Mooney, D.J., 2017. Mechanical forces direct stem cell behaviour in development  
454 and regeneration. *Nat. Rev. Mol. Cell Biol.* <https://doi.org/10.1038/nrm.2017.108>
- 455 Wang, W., Yeung, K.W.K., 2017. Bone grafts and biomaterials substitutes for bone defect  
456 repair: A review. *Bioact. Mater.* <https://doi.org/10.1016/j.bioactmat.2017.05.007>
- 457 Wei, S., Ma, J.X., Xu, L., Gu, X.S., Ma, X.L., 2020. Biodegradable materials for bone defect  
458 repair. *Mil. Med. Res.* <https://doi.org/10.1186/s40779-020-00280-6>
- 459 Zhang, D., Weinbaum, S., Cowin, S.C., 1998. Estimates of the peak pressures in bone pore  
460 water. *J. Biomech. Eng.* 120, 697–703. <https://doi.org/10.1115/1.2834881>
- 461 Zhao, Y.H., Lv, X., Liu, Y.L., Zhao, Y., Li, Q., Chen, Y.J., Zhang, M., 2015. Hydrostatic pressure  
462 promotes the proliferation and osteogenic/chondrogenic differentiation of mesenchymal  
463 stem cells: The roles of RhoA and Rac1. *Stem Cell Res.* 14, 283–296.  
464 <https://doi.org/10.1016/j.scr.2015.02.006>
- 465  
466

467 **FIGURE LEGENDS**

468

469 **Figure 1:** (A) Cyclic hydrostatic pressure device schematics. Hydrostatic pressure was applied  
470 by modulating the pressure in the gas phase above the culture wells in a custom-build pressure  
471 chamber. Air from incubator atmosphere was compressed using a compressor and injected in  
472 the pressure chamber using solenoid valves. (B) Experimental conditions. After 1 week of  
473 proliferation, cyclic hydrostatic pressure stimulation was applied during 1 hour per day, for up to  
474 2 weeks at a frequency 1Hz, oscillating between 0 and 280 kPa with respect to ambient  
475 pressure. The samples were removed from the pressure chamber after each cycle and kept at  
476 ambient pressure between the stimulation phases.

477

478 **Figure 2:** (A) Representative confocal laser scanning microscope image showing seeded cells  
479 scaffolds (scale bar = 100  $\mu\text{m}$  – applies to all). The scaffolds were stained for cellulose (red) and  
480 for cell nuclei (blue). (B) Cellular density after 1 week or 2 weeks of stimulation. Statistical  
481 significance (\* indicates  $p < 0.05$ ) was determined using a one-way ANOVA and Tukey post-hoc  
482 tests. Data are presented as means  $\pm$  S.E.M. of three replicate samples per condition, with  
483 three areas per sample.

484

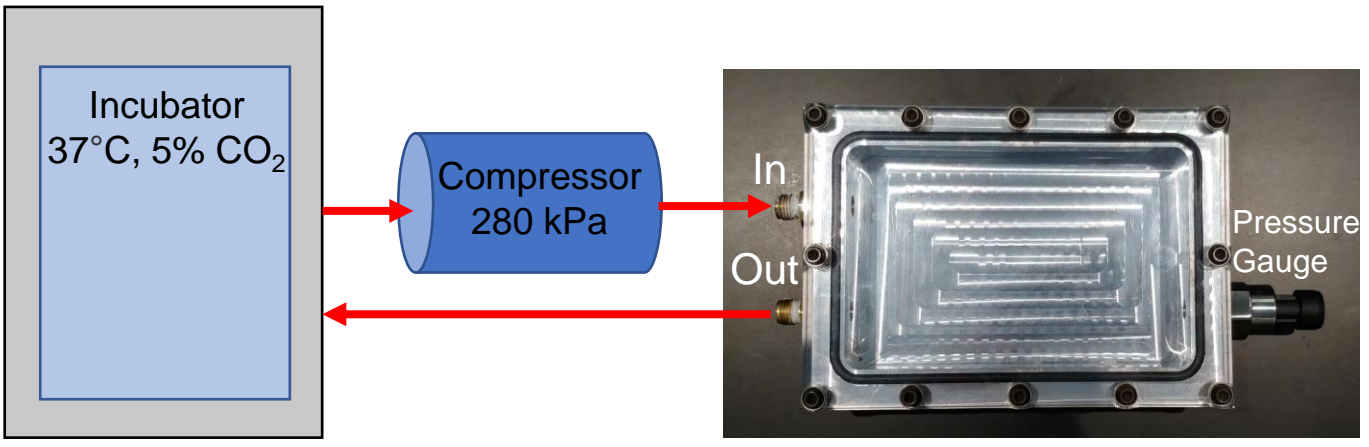
485 **Figure 3:** Alkaline phosphatase (ALP) activity after 1 week or 2 weeks of stimulation. Statistical  
486 significance (\* indicates  $p < 0.05$ ) was determined using a one-way ANOVA and Tukey post-hoc  
487 tests. Data are presented as means  $\pm$  S.E.M. of three replicate samples per condition.

488

489 **Figure 4:** Mineral deposit quantification with Alizarin Red S (ARS) staining after 1 week or 2  
490 weeks of stimulation. Statistical significance (\* indicates  $p < 0.05$ ) was determined using a one-  
491 way ANOVA and Tukey post-hoc tests. Data are presented as means  $\pm$  S.E.M. of three  
492 replicate samples per condition.

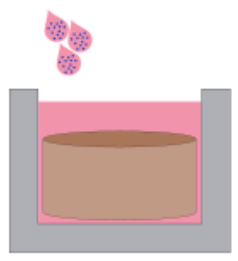
# Figure 1



## A



## B

### Proliferation



 = Culture media  
 = Osteogenic media

### Stimulation

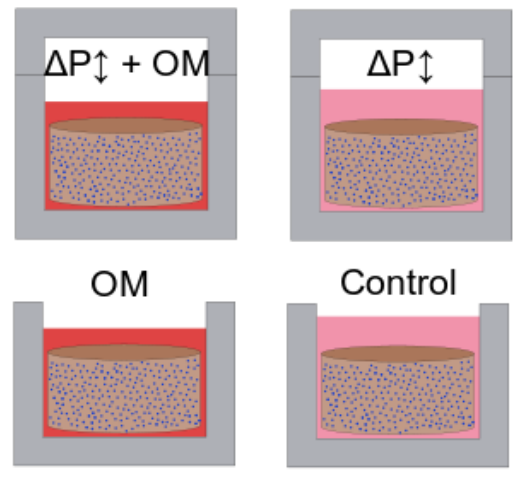
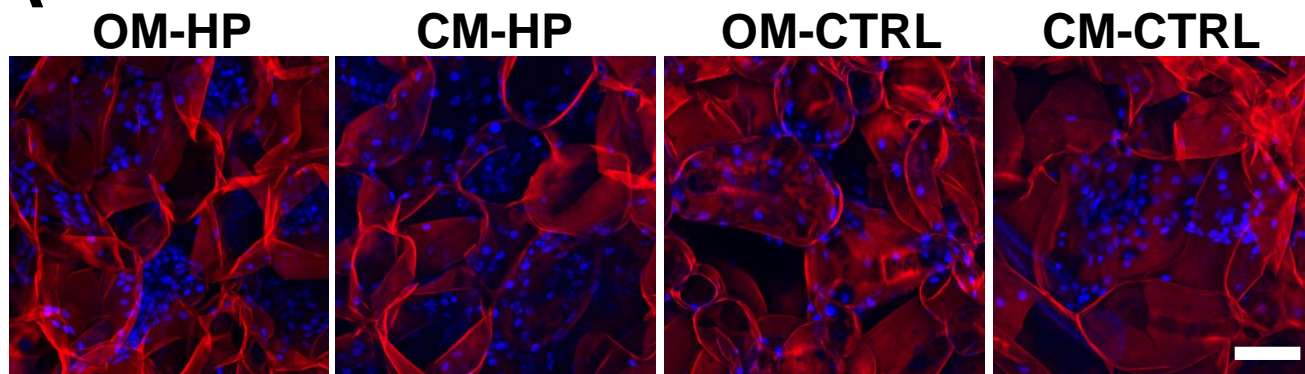


## Figure 2

# A



# B

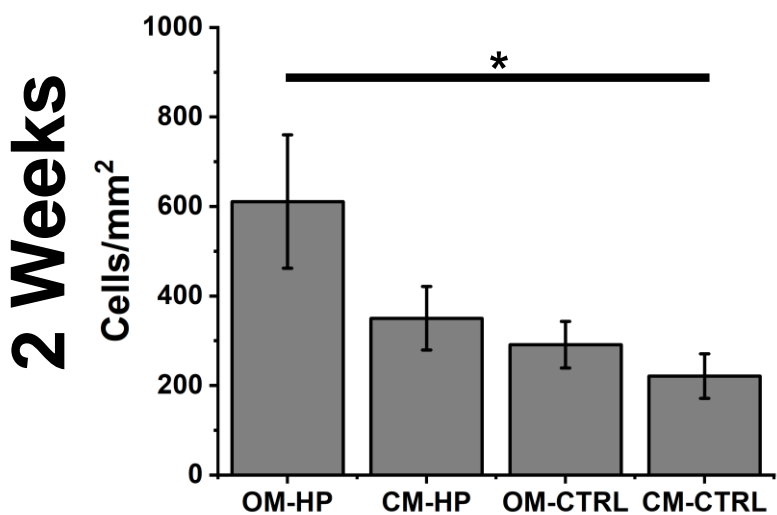
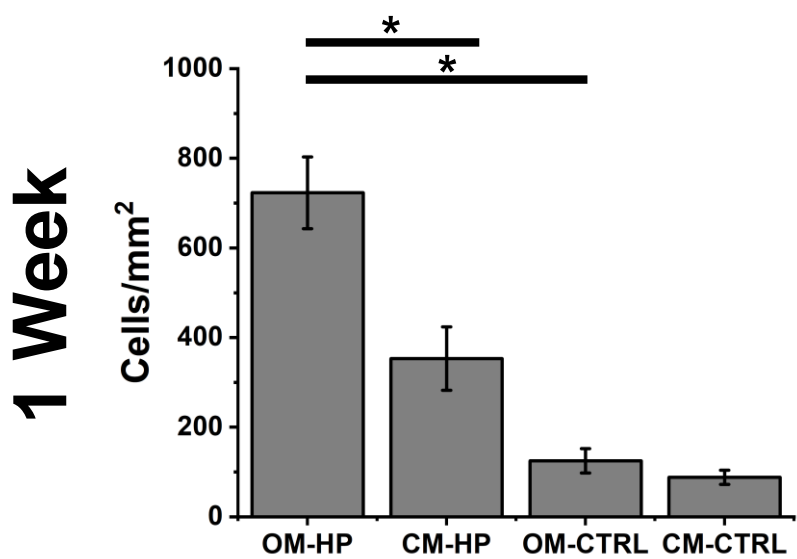


# Figure 3

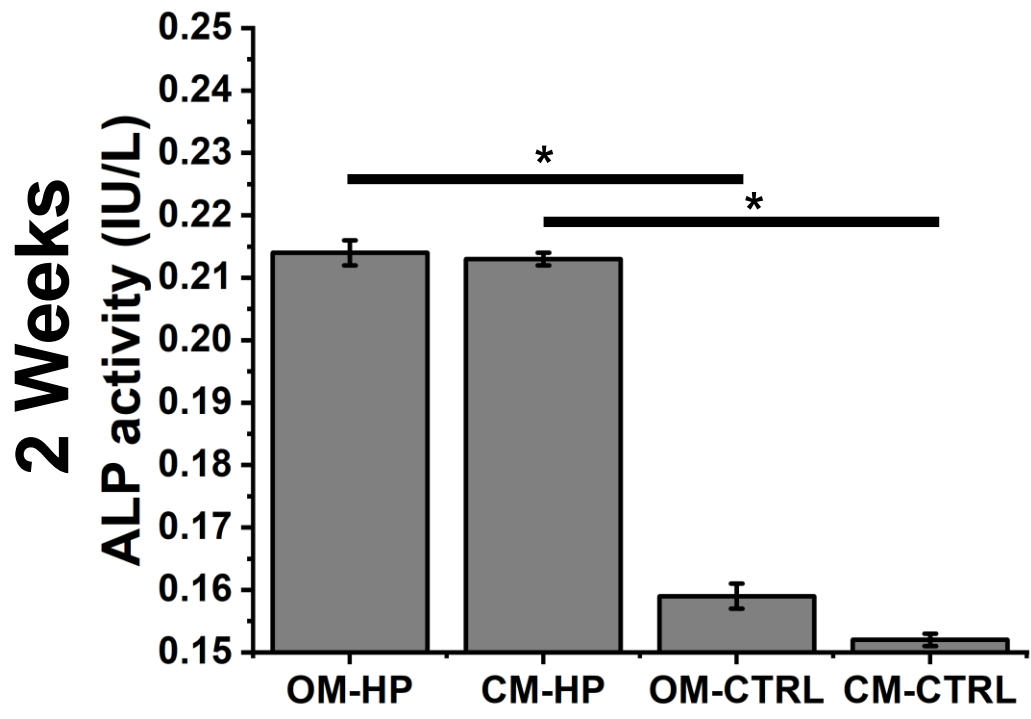
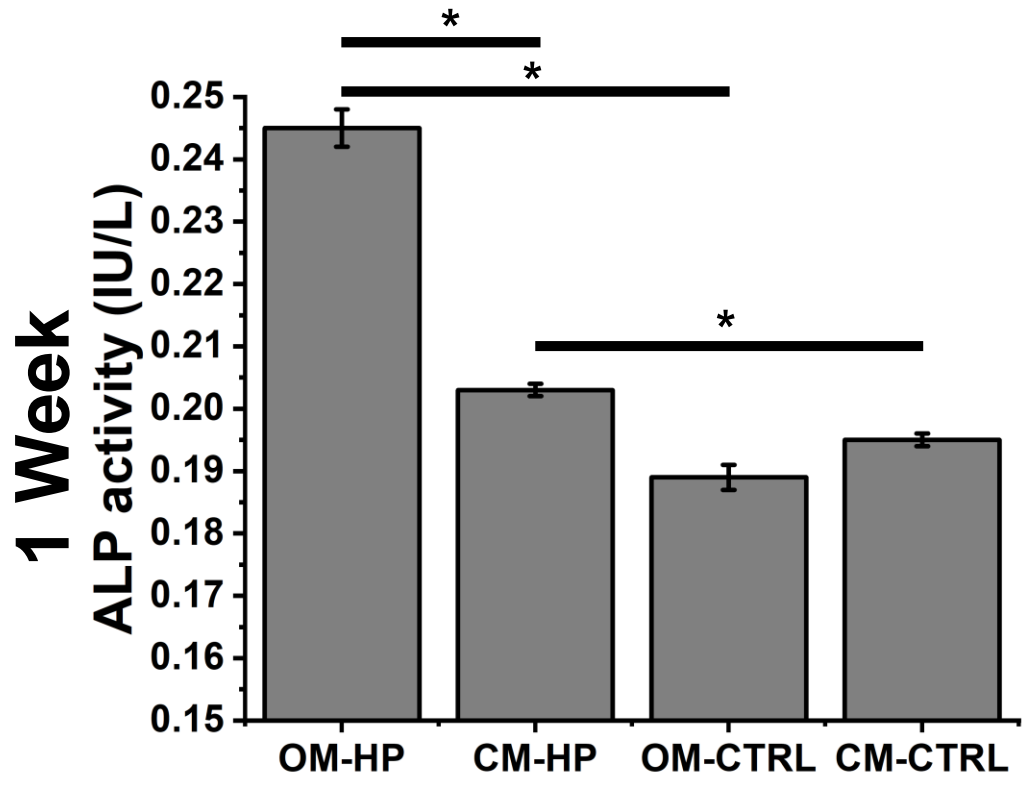
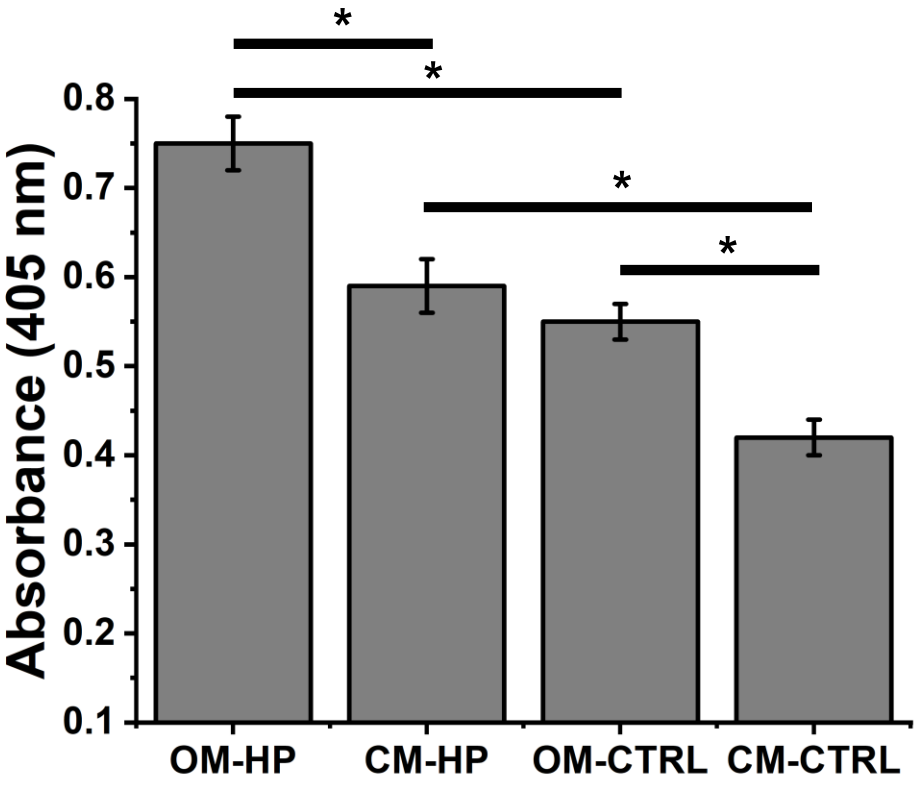


# Figure 4

1 Week



2 Weeks

